sciendo

Nordic Concrete Federation

ISSN online 2545-2819
ISSN print 0800-6377

DOI: 10.2478/ncr-2019-0006

Received: March 31, 2019
Revision received: June 16, 2019
Accepted: June 18, 2019

Clays as SCM – Reactivity of Uncalcined Kaolinite and Bentonite, and Impact on Phase Assemblage and Strength Development of PC Mortars

Mette Rica Geiker, Dr.
Professor, Department of Structural Engineering
Norwegian University of Science and Technology (NTNU)
NO-7491 Trondheim, Norway
mette.geiker@ntnu.no

Emmanuel Gallucci, Dr.
Principle Scientist, Sika Technology AG
Tüffenwies 16
CH-8048 Zürich, Switzerland
gallucci.emmanuel@ch.sika.com

ABSTRACT

The impact of substitution of cement paste with uncalcined clay (bentonite and kaolinite) in the range of 5% by volume of paste on the development of hydration and properties of mortar was investigated. Two issues were addressed, the expected filler effect of the dispersed sub-micron clay particles, and the possible chemical reactivity of the clay.

The study indicated that Portland cement paste may be modified by addition of well dispersed clay and that the impact includes accelerated cement hydration as well as altered distribution of products. Compressive strength development was accelerated, but later age strength was reduced, especially for the bentonite mixes. In contrast, microscopic porosity measurements indicated no detrimental impact on the coarse capillary porosity.

The investigation indicates that for durability related engineering properties, the application of uncalcined clay might be a potential means for reduction of the clinker factor in concrete in support of sustainability.

Key words: Uncalcined clay, cement hydration,

1. INTRODUCTION

By mass, cement is the largest manufactured product on Earth. Because of the increased demand, the emissions due to cement production are increasing. It was in 2016 estimated by some sources to be around 10% of the total anthropogenic CO_2 or about 6% of the total anthropogenic greenhouse gasses [1]. Thus, even relatively small improvements may have a measurable impact. Alternative materials, so-called supplementary cementitious materials (SCMs), have for many years been used to improve and engineer the properties of concrete. During the last decades, SCMs are in addition increasingly used to reduce the amount of Portland clinker in concrete [1, 2].

Lothenbach et al. summarized the impact of SCMs on cement hydration [3]. At early ages, the so-called "filler effect" increases the rate and/or prolongs the Portland clinker reaction. There seems to be two mechanisms of the filler effect: a) apparent higher water-to-cement ratios (w/c): in case of the same water-to-solid ratio, the space for early cement hydration is relatively larger if part of the solid is none or slowly reacting, and b) enhanced nucleation: especially fine filler brings extra surfaces for nucleation. Examples of the mechanisms can e.g. be found in [4, 5]. SCMs react later; their reaction depends on composition, fineness and glassy phases and increases with pH and temperature [3]. Reactive SCMs affects the amount and kind of hydrates formed and thus the engineering properties of the concrete. At normal levels of substitution of silica rich SCMs, the major changes are reduced portlandite and reduced Ca/Si ratio of the calcium-silicate hydrates (C–S–H) [3]. Alumina-rich SCMs increase the aluminate containing hydrates and the aluminium-uptake in C–S–H [3].

Clay particles may increase the cement's reaction rate. The effect of selected layer silicates (kaolinite and bentonite) on the rate of reaction of cement was investigated by Krøyer et al. [6] using ^{29}Si magic-angle spinning (MAS) nuclear magnetic resonance (NMR) on cement pastes (white Portland cement, 10% bentonite or 20% kaolinite by weight of cement, w/c = 0.5) hydrated between 1 and 90 days at 20ºC. They found that the clays increased the rate of cement hydration. The clay addition affected the SiO_4-chains in the C-S-H gel. In average kaolinite caused longer SiO_4-chains to form, whereas bentonite resulted in slightly shorter SiO_4-chains, which at later age increased in length. Using ^{27}Al MAS NMR Krøyer et al. [6] observed similar rate of ettringite formation in pastes with and without kaolinite and that kaolinite was not consumed. The increased rate of cement hydration in pastes with clay was explained by clay particles acting as nucleation sites for the cement hydrates.

Lindgreen et al. [7] focusing on the dispersion of the clay particles in the mix found that addition of micro and nanosized particles to cementitious mixtures may result in a more homogeneous and finer pore structure. This seems mainly to be due to the growth of C-S-H on the clay particle surfaces, where the nanostructure of the C-S-H seems to depend on the size, shape and charge of the clay particles. Based on the observations, they argued that the cement paste structure and porosity can e.g. be engineered by addition of non-pozzolanic layer silicates having specific particle shapes and surface properties (e.g. surface charge and specific surface area).

In addition, both betonite and kaolinite have finer grain size than cement (mean grain size at 300·50·3 nm, and 0.1-1 μm, respectively, compared to cement with a typical main grain size of 10 μm), they will, when well dispersed, affect the packing of the solid particles of the paste in areas where the packing is restricted, i.e. in interfacial zones (ITZ) towards larger particles as coarse aggregates and reinforcement. Some clays adsorb water, the amount depending on the structure of and the ionic layer on the clay. Possible adsorbed water may also affect the final pore structure.

The purpose of the present study was to investigate the effect of uncalcined bentonite and kaolinite clays on the microstructure of Portland cement mortar. Bentonite clay adsorbs water, whereas kaolinite clay according to Lindgreen et al. [7] does not. Two issues were addressed, the expected filler effect of the dispersed sub-micron clay particles, and the possible chemical reactivity of the clay.

2. EXPERIMENTAL

The impact of uncalcined clay was investigated on mortars with 20% or 40% sand by volume and target w/c = 0.50 (Series 1) and w/c = 0.48 (Series 2a) and on pastes with target w/c=0.48 (Series 2b). The clay substituted approximately 5% by volume of cement paste. The bentonite used was found to adsorb 37% water by weight. This was taken into account in Series 1 (by adding a comparable amount of additional water to the bentonite mix), but not in Series 2. Series 1 focused on microstructure and phase assemblage in well hydrated specimens, whereas Series 2 focused on property development.

2.1 Raw materials

The cement was an CEM I 52,5 R - SR5 (according to EN 197-1:2011) white Portland cement from Aalborg Portland A/S, Denmark. The chemical composition of the cement is given in Table 1. The phase composition of the cement is given in Table 2. Selected physical properties are given in Table 3. Due to time difference between undertaking Series 1 and Series 2, two different batches of cement with slightly different properties were used.

The clays were kaolinite and bentonite from English China Clay and Leca, respectively. The chemical composition of the bentonite and the kaolinite is given in Table 1. Bentonite was microcrystalline (60% illite/smectite, 18% illite and 22% kaolinite); the phase composition is given in Table 3. The illite/smectite component had an average thickness of 3 nm with net negative charge and pronounced colloidal properties. Kaolinite is crystalline, almost neutral sized 0.1-1 μm particles with slight colloidal properties. [7] Based on water sorption and suction measurements on the bentonite in artificial pore solution the amount of water adsorbed by the clay in a cement paste was estimated to 37% [8], see Figure 1. The absorption of the kaolinite was according to Lindgreen et al. 0% [7].

The sand was sea sand (Søsand 0-2, kl. E, SA-Storebæltsand). The grading of the sand is given in Table 5.

For Series 2, Sika® Viscocrete PC2 was used as superplasticizer and Sika® Stabilizer-4R was used as stabilizer.

Table 1 - Oxide composition and loss on ignition (LOI) of cement (Series 1 (S1) [4], Series 2 (S2) own measurements) and the bentonite and kaolinite clays [6], LOI Series 2 own measurements.

Raw material	SiO_2	Al_2O_3	Fe_2O_3	CaO	MgO	SO_3	TiO_2	K_2O	Na_2O	MnO	P_2O_5	LOI [a]
Cement (S1)	24.7	2.1	0.4	68.7	0.6	1.8	0.1	0.1	0.2	0.0	0.5	1.0
Cement (S2)	24.1	2.6	0.5	68.9	0.7	2.2	0.1	0.1	0.2	0.0	0.3	1.0
Bentonite	55.2	19.3	8.3	0.9	2.8	0.9	0	0.9	3.7	-	-	8.0 (11.5)
Kaolinite	68.8	18.6	1.6	0.3	0.7	-	1.2	2.1	0.2	-	-	6.7 (6.3)

Note a: Series 2 in brackets

Table 2 - Phase composition of cement. Series 1 [4]; Series 2 own measurements.

	C_3S	C_2S	C_3A	C_4AF	$C\bar{S}\cdot 2\,H$	$C\bar{S}\cdot \frac{1}{2}\,H$	$C\bar{S}$	CH
Series 1	68.1	23.6	3.6	0	0	0.5	2.9	0.5
Series 2	70.6	20.3	3.1	0.3	2.1	1.0	0.2	1.2

Note: No traces of lime C, periclase M, arcanite $K\bar{S}$ or calcite $C\bar{C}$

Table 3 - Selected physical properties of cement and clays [7].

Property	Unit	Cement	Bentonite	Kaolinite
Mean grain size	μm	d50=10	Laths, thickness 0.003 width ~0.1 length 0.1 – 0.5	Platy; thickness 0.005-0.05 width 0.005-0.05
Specific surface	m^2/kg	397	79.000	19.000
Density	kg/m^3	3135	2600	2600
Absorption	%	-	37	0

Table 4 - Phase composition of clays.

	Quartz	Muscovite 2M	Muscovite 3T	Dickite	Illite	Amorphous
Kaolinite	52.1	19.1	0.3	24.1	-	4.5
Bentonite	3.8	39.0	-	11.5	2.0	43.7

Table 5 - Grading of sand (% passing).

Sieve size, mm	0.075	0.125	0.25	0.5	1	2
Series 1 and 2	0.2	0.5	14.4	74.7	97.3	100

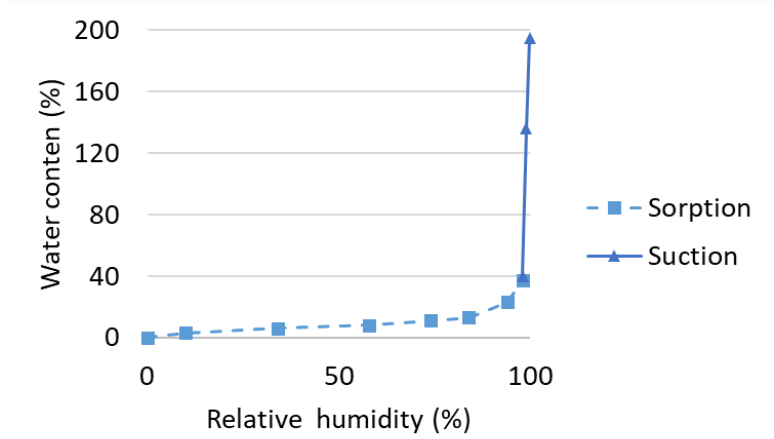

Figure 1 – Sorption and suction isotherm for bentonite in artificial pore fluid, after [8].

2.2 Mix designs, casting and curing

Mortars with the compositions given in Table 6 and Table 7 (Series 1 by volume and weight), and Table 8 (Series 2 by weight), and pastes with the compositions given in Table 9 were prepared. The mix id includes abbreviations of the binder (R: Cement (reference); K: Cement plus kaolinite, B: Cement plus bentonite) and the volume fraction of sand. In the preparation of the specimens, the dispersion of the layer silicates in the mixtures was carefully considered. The clays were added as suspensions, premixing the clay with water for 24 hours to facilitate dispersion [9]. The free water includes the LOI of the clays, but excludes water adsorbed in bentonite (37%). For Series 1, the free water content by weight of cement is comparable, while for Series 2, the total water content by weight of cement is comparable.

Series 1
Series 1 was prepared with target w/c = 0.50, the actual w/c includes unexpected water (LOI, Table 1) in the clays. Mixing of Series 1 was undertaken in a custom-made 2 litres container by means of custom-made mixer. The clays were dispersed by premixing the clays with mixing water; the ratio was either 1:2.5 or 1:4. Bleeding was not observed except a faint bleeding for the reference. Specimens were stored in closed plastic containers, which were kept in a water saturated atmosphere at room temperature to limit long-term evaporation and carbonation reactions.

Table 6 - Mortar compositions, Series 1 (volume fractions).

Mix	Cement	Kaolinite	Bentonite incl. ads. water	Sand	Ads. water in clay	Free water	Total water
R_20	0.310	0.000	0.000	0.20	0.000	0.490	0.490
B_20	0.293	0.000	0.037	0.20	0.025	0.468	0.493
K_20	0.294	0.037	0.000	0.20	0.000	0.470	0.470
R_40	0.233	0.000	0.000	0.40	0.000	0.368	0.368
B_40	0.219	0.000	0.028	0.40	0.018	0.350	0.369
K_40	0.220	0.028	0.000	0.40	0.000	0.353	0.353

Table 7 - Mortar compositions, Series 1 (weight per kg cement).

Mix	Cement	Kaolinite	Bentonite incl. ads. water	Sand	Ads. water in clay	Free water	Total water
R_20	1.000	0.000	0.000	0.536	0.000	0.500	0.500
B_20	1.000	0.000	0.099	0.575	0.027	0.506	0.533
K_20	1.000	0.104	0.000	0.564	0.000	0.507	0.507
R_40	1.000	0.000	0.000	1.430	0.000	0.500	0.500
B_40	1.000	0.000	0.099	1.533	0.027	0.506	0.533
K_40	1.000	0.104	0.000	1.505	0.000	0.507	0.507

Series 2

Mortars were mixed according to EN 196-1 [10]. The batch size corresponded to approximately 2.5 kg cement. The clays were dispersed by premixing the clays with mixing water; bentonite with all mixing water, kaolinite with half. Table spread flow was measured immediately after mixing and 100 g of mortar were used for isothermal calorimetry. For each of those mix designs, 12 40·40·160 mm^3 prisms were cast according to EN 196-1 for compressive strength testing, two per testing age. The prisms were kept in moulds during the first 24 hrs, 2 prisms were immediately tested after demoulding for the 1 day properties, and the others were stored in climatic chamber at 23°C under 95% relative humidity (RH).

Pastes were mixed using a Heidolph mixer at 2000 rpm for 2 min. The batch size corresponded to approximately 100 g cement.

Table 8 - Mortar compositions, Series 2a (weight per kg cement).

Mix	Cement	Kaolinite	Bentonite incl. ads. water	Sand	Stabilizer 1)	Super-plasticizer 1)	Ads. water	Free water 2)	Total water
R_40	1.000	0.000	0.000	1.430	0.001		0.000	0.480	0.480
B_40	1.000	0.000	0.098	1.533		0.002	0.026	0.464	0.490
K_40	1.000	0.104	0.000	1.505		0.001	0.000	0.488	0.488

1) Excluding water
2) Including water in admixtures

Table 9 - Paste compositions, Series 2b (weight per kg cement).

Mix	Cement	Kaolinite	Bentonite incl. ads. water	Stabilizer 1)	Super-plasticizer 1)	Ads. water	Free water 2)	Total water
R_40	1.000	0.000	0.000	0.001	-	0.000	0.480	0.480
B_40	1.000	0.000	0.098	-	0.002	0.026	0.464	0.490
K_40	1.000	0.104	0.000	-	0.001	0.000	0.488	0.488

1) Excluding water
2) Including water in admixtures

2.3 Methods

An overview of the investigations undertaken on the hardening and hardened specimens is given in Table 10. In addition, the workability of mortars in Series 2 was characterized. The development of hydration was determined by calorimetry up to 2 days and X-ray diffraction (XRD), thermogravimetry (TGA) and scanning electron microscopy (SEM) at later age. The microstructure was investigated using SEM and low temperature calorimetry (thermoporometry, LTC). Strength development was determined on mortar prisms.

SEM of the paste and mortar specimens prepared in Series 1 showed that only the mortars with 40 % sand had an acceptable homogeneity for quantitative analysis, indicating an inefficient mixing of pastes and of mortars with 20 % sand. The pastes and the mortars with 20 % sand were therefore only used for determination of the chemical composition.

Fresh concrete properties, spread
The consistency of the mortars in Series 2 was determined using an automated shocking spread flow table according to EN 1015-03 [11].

Table 10 - Overview of investigations on hardening and hardened specimens. S1 and S2 refer to Series 1 and Series 2. XRD: X-ray diffraction, TGA: thermogravimetry, SEM: scanning electron microscopy; LTC: low temperature calorimetry.

Binder	Material	Id	Calorimetry	XRD	TGA		SEM		LTC	Strength
			0-2 days	1, 3, 7, 21, 35, 70 days		7 days	35 days	120 days	120 days	1, 3, 7, 21, 35, 113 days
Cement (R)	Paste	R_0		S2	S2	S1	S1			
	Mortar, 20% sand	R_20				S1	S1	S1		
	Mortar 40% sand	R_40	S2					S1	S1	S2
Cement plus bentonite (B)	Paste	B_0		S2	S2	S1	S1			
	Mortar, 20% sand	B_20				S1	S1	S1		
	Mortar 40% sand	B_40	S2					S1	S1	S2
Cement plus kaolinite (K)	Paste	K_0		S2	S2	S1	S1			
	Mortar, 20% sand	K_20				S1	S1	S1		
	Mortar 40% sand	K_40	S2					S1	S1	S2

Calorimetry
Development of hydration was measured by isothermal calorimetry on 100 g mortar specimens (Series 2) using and ICal 8000 device from Calmetrix. Hydration kinetics were followed continuously from right after mixing until 48 hours.

X-ray diffraction (XRD)
Phase assemblage of raw materials and hydrated specimens was measured using X-ray diffraction XRD D8 advance device from Bruker, and calculated through Rietveld analysis using Bruker Topas 5.0. Amorphous content was always back calculated using an external standard strategy

and pure metallic silicon as standard. Raw materials were measured as received while hydrated specimen were measured on hardened pastes which hydration was stopped at desired ages through solvent exchange in isopropyl alcohol, then dried at low temperature and ground.

Thermogravimetry (TGA)
TGA diagrams were acquired using a Netzsch TG209 F1 Libra device at a heating rate of 10°K/mn and under constant flow of pure nitrogen. For each measurement, 15 to 20 mg of specimen were used and measurements were run in alumina crucibles. Raw materials were processed as provided while hydrated paste specimens were evaluated after isopropanol exchange and oven drying as described in the XRD section.

Scanning electron microscopy (SEM)
Prior to scanning electron microscopy (SEM) investigation, vertical slices of around 5 mm thickness were cut in the specimens at given ages (Table 10) and dried by solvent exchange in isopropyl alcohol for one week. The slices were then epoxy impregnated (epotek 301) and softly polished with decreasing grades of diamond crystallites. Backscattered Electron Imaging was done at 15 kV with FEI Quanta 200 SEM. EDS elemental characterisation was done with a PGT SiLi detector using pure standard minerals.

Low temperature calorimetry (LTC)
Cylindrical specimens of mortar (40% sand, Series 1) with diameter of 15 mm and a length of 70 mm were used. The specimens were vacuum saturated prior to testing according to NT Build 492 [12]. Excess liquid was removed with a damp cloth. After low temperature calorimetry (LTC) the specimens were dried at 105°C ± 5°C until constant weight was achieved (± 0.1°C) to determine the total water content of the specimens.

The LTC measurements were performed in a low temperature Calvet Micro Calorimeter, model "–196°C to 200°C", from Setaram [13,14]. Temperature cycles were made between +20°C and minimum –48°C. The cooling and heating rates were –3.3°C/h and +4.1°C/h, respectively. No nucleation agent was used. The measured temperatures were registered in the reference block. The heat flow is given as the apparent heat capacity; calculated using the method of Sellevold and Bager [15].

Mechanical testing
Compressive strength testing was undertaken on mortar prisms with 40% sand (Series 2) according to EN 196-1 [10], two prisms were tested for flexural strength and the obtained four half prisms were tested for compressive strength and testing was undertaken after 1, 3, 7, 21, 35 and 113 days in a high humidity climate chamber.

The air content of mortars was determined in accordance with [16] on the basis of the density of theoretically air void free mortar and the weight at testing. The compressive strength was normalized to an air content of 2 vol % using Bolomey's equation, e.g. [16].

3. RESULTS AND DISCUSSION

Addition of kaolinite and bentonite changed the colour of the white Portland paste and mortar from white/light grey to brownish and dark, respectively. The clay addition also affected the consistency of the fresh mortars, which is illustrated by the need for superplasticizer to obtain

comparable spread (Table 8). Furthermore, despite similar spread right after mixing, the spread 30 min after mixing was significantly lower in the case of the kaolinite mix compared to the reference, see Figure 2. The reduced consistency of the clay mixes is expected to have affected the degree of compaction of the mortars, which is indicated in the air content calculated based on the difference between theoretical and measured densities of the prisms cast in Series 2 (average calculated air content 1.3%, 3.8% and 2.8% for the reference, bentonite and kaolinite mortar prisms).

Figure 2 - Spread of mortar (Series 2) 30 min after mixing; left: reference; right: kaolinite.

Compressive strength development of mortars with 40 % sand (Series 2) is shown in Figure 3; both as measured and when calculated to constant (2%) air content. The coefficient of variation was 1-7%. Both kaolinite and bentonite are observed to enhance the early age strength development, whereas the strength at later age appears compromised, especially when substituting cement paste with the bentonite. It should be noted that the bentonite used was found to adsorb 37% water by weight. This was not taken into account in Series 2, see Table 8.

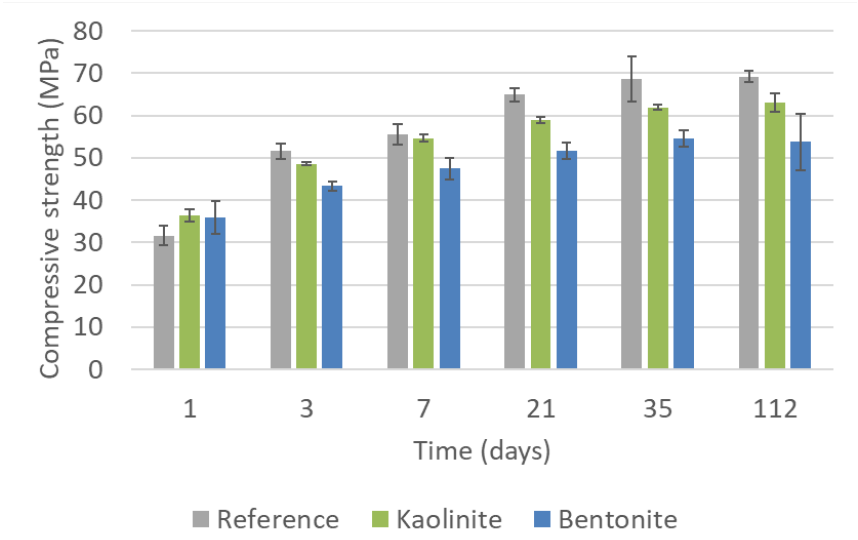

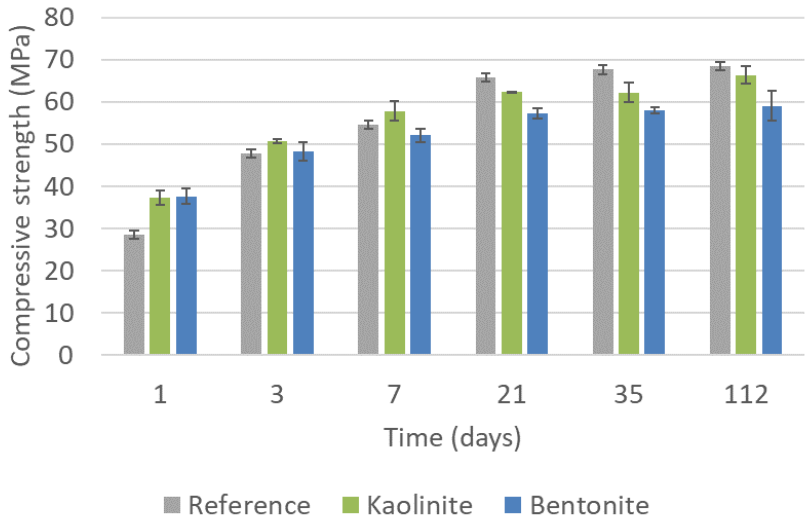

Figure 3 - Development of compressive strength of mortar prisms (Series 2); top) as measured, bottom: recalculated to 2% air content in mortars. The error bars mark the standard deviation.

The impact of the clay addition on the early hydration is illustrated in Figure 4. Both clays are observed to cause an earlier start of the acceleration period and a higher maximum heat flow of the aluminates peak (second peak in the acceleration period, bentonite slightly more than kaolinite. Considering the two mechanisms for filler effects described in [3]: a) increased space causing prolonged hydration and b) increased nucleation sites causing acceleration, the effect of the clays are in theses mixes enhanced nucleation. This is according to expectations considering the large surface area of the clays.

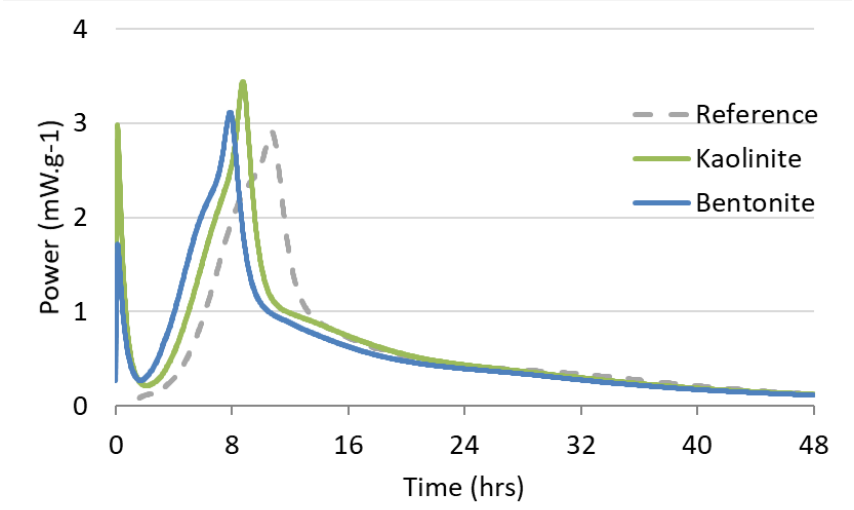

Figure 4 - Development of early hydration as a function of time determined by calorimetry of mortars (Series 2) hydrated sealed at 20°C. The data are normalized to weight of mortar.

Two issues are addressed: the expected filler effect of the clay particles and the possible chemical reactivity of the clay.

Filler effect of bentonite and kaolinite
Both bentonite and kaolinite had a filler effect on the hydration of the cement. A shorter induction period and an increased reaction rate in the acceleration period (nucleation rate) were observed by calorimetry (Figure 4).

The observations were confirmed by XRD. Figure 5 shows the degree of hydration (DoH) measured form normalized content of C_3S, C_2S, C_3A and calcium sulphate. (C_4AF not taken into account since present in very little amount and probably not reactive). The impact of clays at early age is clearly visible with a lower DoH for cement and higher DoH for bentonite, in agreement with hydration kinetics measured by calorimetry. At later ages the differences level out. Most probably, higher DoH of bentonite at 70 days is mainly due to a sudden drop of belite content as measured by XRD and is most likely caused by an artefact.

The observed filler effect of the clays is in agreement with ^{29}Si MAS NMR data [6]. They found that bentonite and kaolinite accelerated the hydration of alite and belite. However, using ^{27}Al MAS NMR Krøyer et al. [6] did not observe a corresponding filler effect of kaolinite clay on the reactions of the aluminate phases (bentonite clay was not investigated due to the impact of iron on the aluminium spectrum).

The accelerating effect of the clays might be explained by either a) higher ionic concentrations due to reduction of available water upon adsorption by the clays or b) more surface available for nucleation of hydrates.

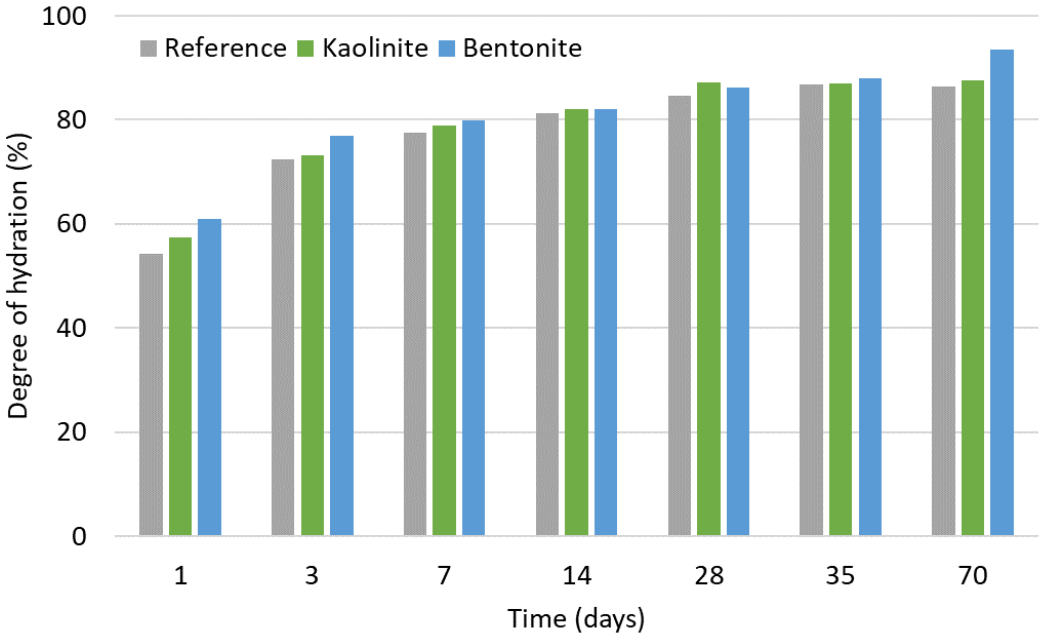

Figure 5 - Development of hydration as a function of time of pastes hydrated at 23°C and 95% RH (remains of C_3S, C_2S, C_3A, and calcium sulphate determined by XRD and Rietveld analysis).

A qualitative microstructural description is obtained from micrographs of the 120 days old specimens (Figure 6). The systems were highly hydrated as only belite and large alite grains remained unhydrated. At the used resolution, the microstructure of the hydrated systems was not much affected by the clays: same patterns for calcium hydroxide (CH) precipitates, same

morphology of C-S-H “blobs”, and similar pore morphology are observed. Also, the ITZ was apparently not affected as much CH was observed.

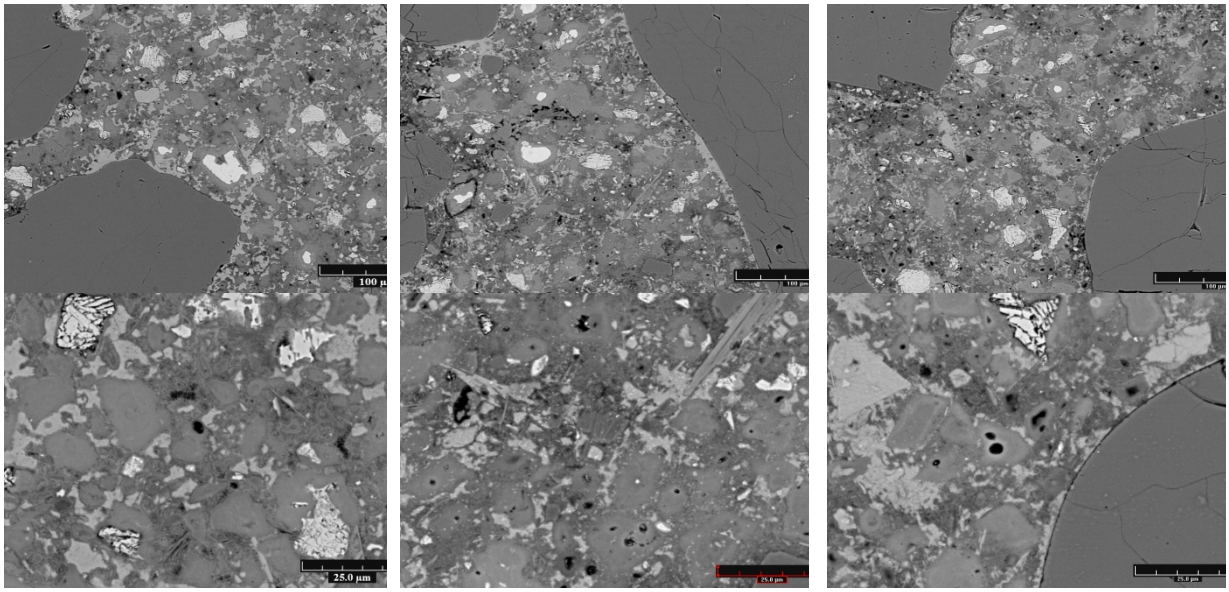

Reference Bentonite Kaolinite

Figure 6 - Micrographs of highly hydrated systems (120 days old mortars, 40% sand, Series 1). Width: Upper 0.5 mm, lower 0.1 mm.

Figure 7 shows that the substitution of cement paste by betonite and kaolinite clays had nearly no impact on the long-term coarse capillary porosity, whereas the presence of clay appears beneficial at early age. Capillary pores were measured by image analysis down to a size of 350 nm. The data given in Figure 7 are normalised to the content of paste and the error bars indicate ± one standard deviation. Also, the substitution of cement paste by bentonite and kaolinite clays had limited impact on ice formation (threshold pores and percolated pore volume) in well hydrated systems, see Figure 8. The measured differences in total freezable water are within observed variations between similar samples [17]. Freezing in the clay samples started at relatively higher temperature, indicating less super-cooling (facilitated ice nucleation). The apparent higher amount of freezable water detected in the high temperature range might indicate larger volumes of percolated pores and possibly larger volumes of coarser pore sizes. The microscopic observations (Figure 6) appears to be in contradiction to the lower compressive strength observed for the Series 2 mortars containing clay (see Figure 3); the low temperature calorimetry data are non-conclusive. It should be noted that the measured water adsorption by bentonite (37% water by weight) was taken into account in the mix design for Series 1, but not for Series 2, which should favour the performance of the bentonite mix in Series 2 compared to Series 1.

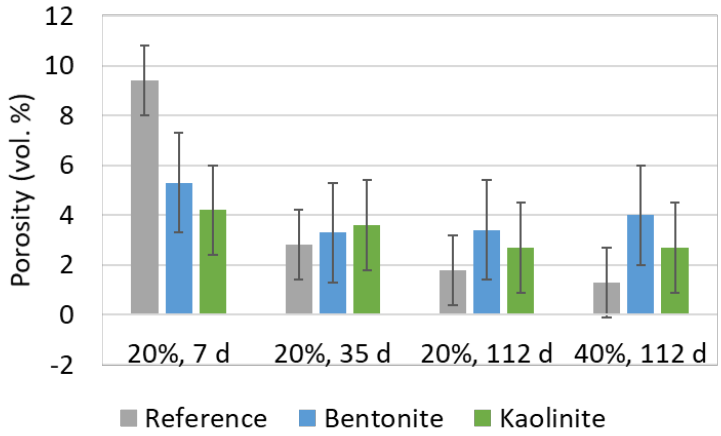

Figure 7 - Capillary porosity (> 350 nm) measured by image analysis on mortars (Series 1). The standard deviation was 0.5-2 vol. %. The error bars mark the standard deviation.

Pozzolanic reactivity of bentonite and kaolinite

Krøyer et al. [6] found by ^{29}Si MAS NMR that the bentonite and the kaolinite clays were not consumed during cement hydration. In contrast to this, we observed at 35 days, the assemblage of phases in equilibrium differs between pure Portland cement (PC) mortar or blend with bentonite and kaolinite clays (Figure 9). In the pure PC mortar, the matrix is mainly a mixture of calcium hydroxide (CH), C-S-H (C-S-H and CH are not marked on the plot but are theoretically at the origin position (no sulphur and no aluminium) and ettringite (Aft) (trend of the grey EDS spot analysis along the line C-S-H / Aft) while in the case of the presence of clay systems, the aluminate phase in equilibrium with C-S-H and CH is calcium monosulfoaluminate (AFm) (scattered blue and green points along the line C-S-H / AFm). This difference in the stability of the AFt vs AFm is probably due to excess aluminate ions brought in the system by the clays and which thermodynamically stabilise the AFm.

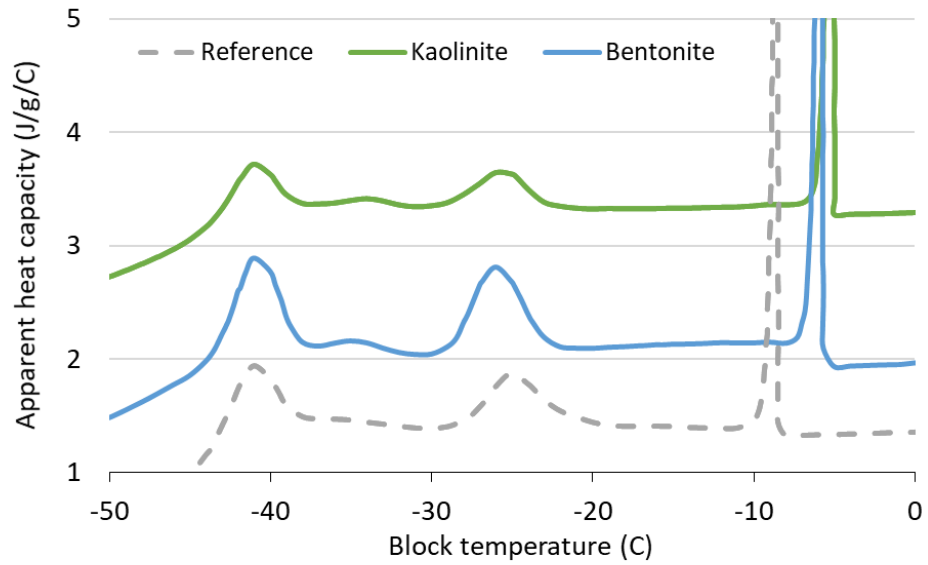

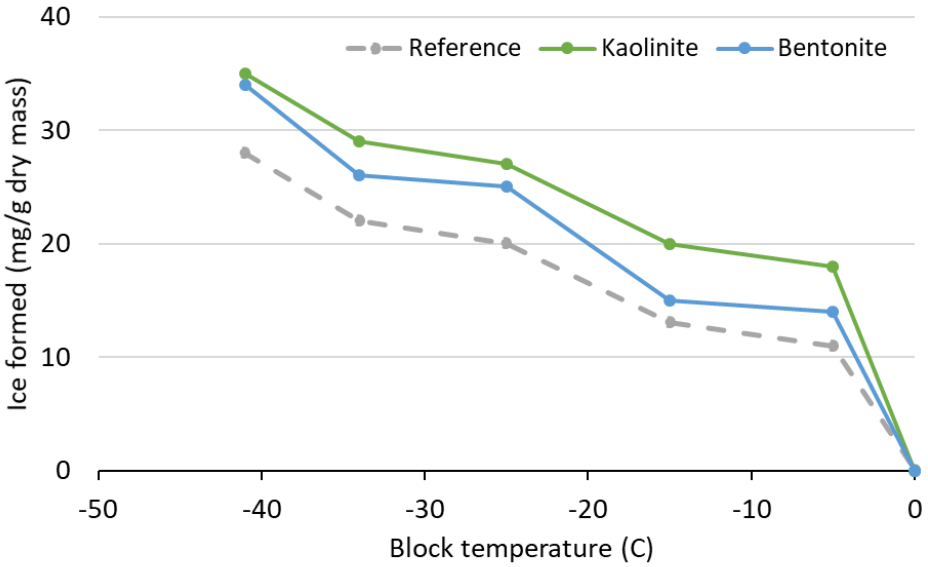

Figure 8 - Threshold pores (upper graph) and ice formation (lower graph) determined by low temperature calorimetry on 120 days old mortars (40% sand, Series 1).

Figure 10 shows that while the pure PC mortar (grey points) had equilibrium between C-S-H, CH and eventually a bit of AFm/AFt, the clay systems had a strong dispersion of the data towards Al and Si rich regions. This is explained by a fine intermixing between C-S-H and the clays at the micron level. In agreement with the composition of the two clays, the trends of the blue and green points vary slightly from each other with the bentonite system tending towards Si richer assemblages while the kaolinite system tends towards an Al richer phase.

The composition of the inner-C-S-H was measured in thick homogeneous rims around unreacted cement grains (or in the place of totally reacted grains) to avoid the intermixing with other phases. The Ca/Si or Ca/(Si+Al) ratios as well as the level of substitution of Si by Al are not affected at all by the presence of the clays in the concerned mixes compared to the reference mortar (Figure 11). This shows that a) if a pozzolanic reaction of the clays has started, it is not developed enough to affect the composition of the so-called inner-C-S-H (or HD-C-S-H); and b) that even if the clays have slightly decomposed (which is supported by observations of Al brought by the clays to the phase assemblage of the matrices, see Figure 9), this does not affect the inner-C-S-H (no change in the Al content).

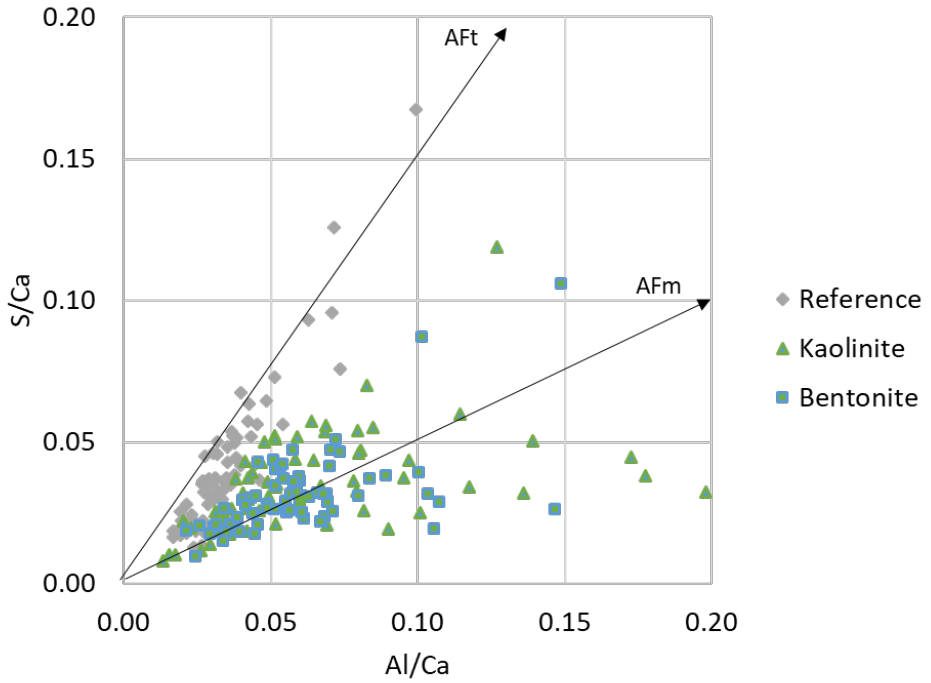

Figure 9 - S/Ca ratio versus Al/Ca ratio of the outer products in 35 days old systems (mortar 20% sand, Series 1). The lower graph is a zoom of the upper.

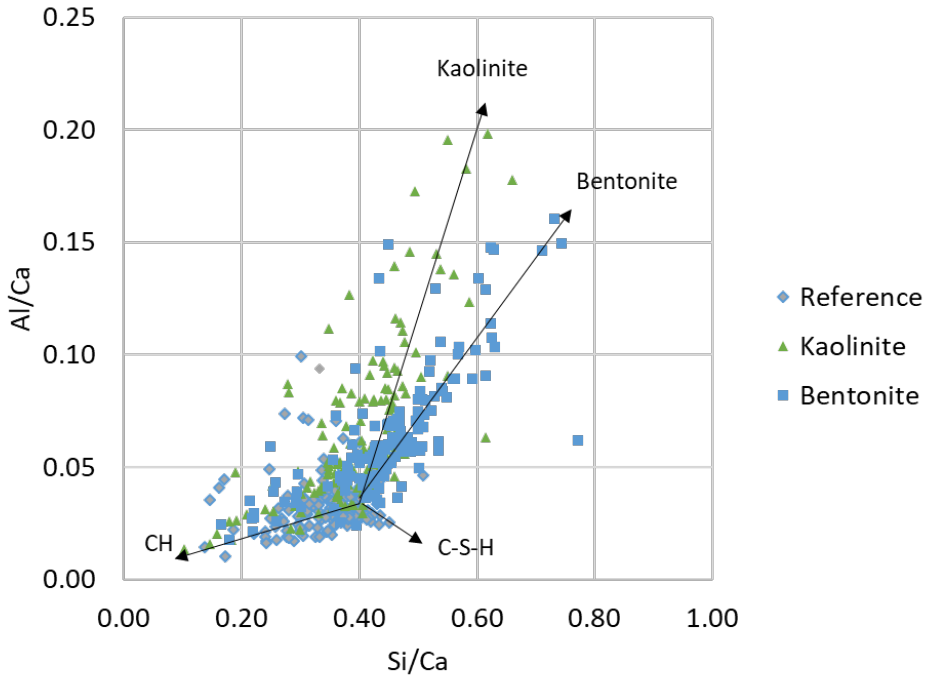

Figure 10 - Al/Ca ratio versus Si/Ca ratio of outer products in 35 days old mortars (20 % sand, Series 1).

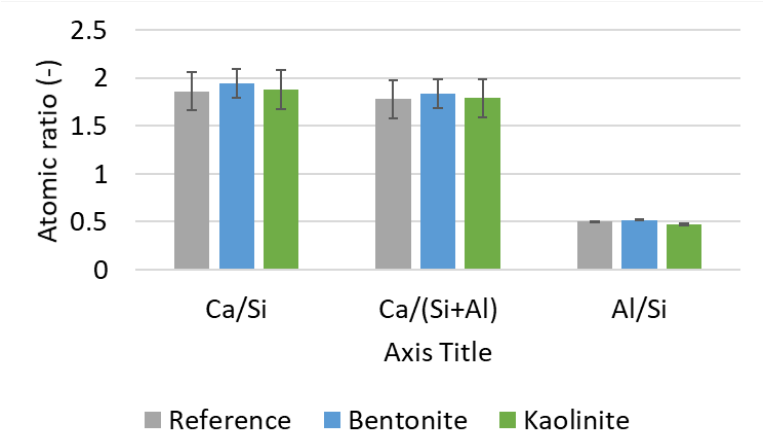

Figure 11 - Composition of inner-C-S-H measured in thick homogeneous rims around unreacted cement grains (112 old mortar specimens with 40% sand, Series 1). The standard deviation was approx. 0.05 for Ca/Si and Ca/(Si+Al); approx. 0.02 for Al/Si.

The pozzolanic activity of the clays has been roughly assessed with the evolution of the CH content in each system (Figure 12). The results given in Figure 12 were renormalized to 140 g of paste (those are not percent). The TGA data for the clay specimens at 35 and 70 days were affected by minor carbonation, which was corrected for assuming all carbonation came from CH. The CH content in the clay specimens appears at later age slightly lower than the CH content in the reference. This might indicate pozzolanic reactivity of the uncalcined clays.

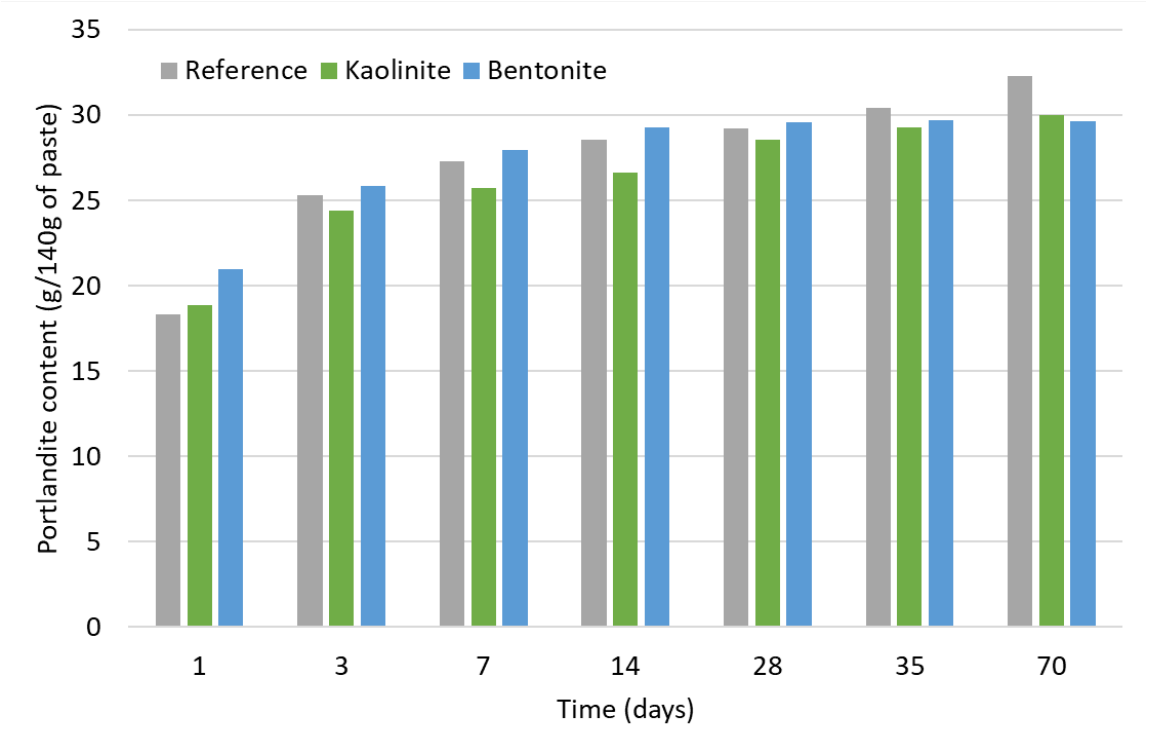

Figure 12 - Portlandite content determined by TGA, paste specimens (Series 2).

4. CONCLUSIONS

The impact of substitution of cement paste with uncalcined clay in the range of 5% by volume of paste on the development of hydration and properties of mortar was investigated. Two issues were addressed, the expected filler effect of the dispersed sub-micron clay particles, and the possible chemical reactivity of the clay.

Well dispersed uncalcined bentonite and kaolinite clays were observed by calorimetry and XRD to have a filler effect increasing early cement reactions; this explains a measured higher early strength development mortars with clay. In combination with observations of clay intermixed with outer C-S-H this indicates that the clays act as nucleation sites; i.e. have a filler effect.

SEM-EDS indicated a fine intermixing of clay and outer hydration products, the inner products were unaltered. Observations of phase assemblages in the clay systems towards AFm instead of AFt indicated some decomposition of the clays. Measurement of portlandite consumption by TGA also indicated potential pozzolanic reactivity of the uncalcined clays.

Replacement of cement paste by clay keeping the free water-to-cement ratio (w/c) constant (Series 1) appeared to lead to unaltered large capillary porosity in the well hydrated systems. In contrast, replacement of cement paste by clay keeping the total water-to-cement constant (Series 2) led to reduction of later strength, especially for the mortar with bentonite. This indicates that the addition of uncalcined alters the porosity reducing compressive strength, but not necessarily durability related properties. The investigations calls for more detailed porosity and durability studies.

5. ACKNOWLEDGEMENTS

The first author would like to thank the Danish Technical Research Council (STVF project 2020-00-0005) and Professor Karen Scrivener, EPFL, Switzerland, for financial support. Also Senior Scientist Holger Lindgreen, GEUS, and Associate Professor Jørgen Skibsted, iNANO, NMR Centret, Aarhus Universitet, are thanked for the collaboration.

6. REFERENCES

1. Scrivener KL, John VM, Gartner EM: “Eco-efficient cements. Potential, economically viable solutions for a low-CO_2, cement-based materials industry.” In United Nations Environment Program, Paris, France, 2016, 64 pp.
2. Damtoft JS, Lukasik J, Herfort D, Sorrentino D, Gartner EM: ”Sustainable development and climate change initiatives”. *Cement and Concrete Research*, Vol. 38, No. 2, 2008, pp. 115-127.
3. Lothenbach B, Scrivener K and Hooton RD: “Supplementary cementitious materials”. *Cement and Concrete Research*, Vol. 41, No. 12, 2011, pp. 1244-1256.
4. Kocaba V: “Development and evaluation of methods to follow microstructural development of cementitious systems including slags”, PhD thesis, EPFL-TH4523, EPFL, Laboratoire des Matériaux de Construction, Lausanne, Switzerland, 2009, 263 pp.
5. Fernandez Lopez R: “Calcined clayey soils as a potential replacement for cement in developing countries”. PhD thesis, EPFL-TH4302, EPFL, Laboratoire des Matériaux de Construction, Lausanne, Switzerland, 2009, 178 pp.

6. Krøyer H, Lindgreen H, Jakobsen HJ, Skibsted J: "Hydration of Portland cement in the presence of clay minerals studied by 29Si and 27Al MAS NMR spectroscopy". *Advances in Cement Research*, Vol. 15, No. 3, 2003, pp. 103-112.
7. Lindgreen H, Geiker M, Krøyer H, Springer N, Skibsted J H: "Microstructure engineering of Portland cement pastes and mortars through addition of ultrafine layer silicates". *Cement and Concrete Composites*, Vol. 30, No. 8, 2008, pp. 686-699.
8. Kjeldsen AM: "New Concretes through addition of layer silicates. Bentonite clay soprtion." *Personal communication*, 2003.
9. Lindgreen HB, Jakobsen HJ, Geiker MR, Stang H, Krøyer H, Skibsted JB: "*Suspension of clays in water for addition to e.g. concrete*". Patent WO2008052554A1, 2008-05-08.
10. EN 196-1. Methods of testing cement - Part 1: Determination of strength, 2005.
11. EN 1015-03. Determination of consistence of fresh mortar (by flow table), 2004
12. NordTest, NT Build 492, "Concrete, mortar and cement-based repair materials: chloride migration coefficient from non-steady-state migration experiments", approved 1999-11.
13. Fontenay le Sage de C, Sellevold EJ: "Ice formation in hardened cement pastes – I. Mature water-saturated pastes", Durability of building materials and components, ASTM STP 691, 1980.
14. Bager D & Sellevold EJ: "Ice formation in hardened cement paste, Part I – Room temperature cured pastes", *Cement and Concrete Research*, Vol. 16, 1986, pp. 709–20.
15. Sellevold EJ & Bager D: "Low temperature calorimetry as a pore structure probe", Proceedings, 7th International Congress on the Chemistry of Cement, Paris, vol. 4; 1981.
16. Osbæck B: "The influence of air content by assessing the pozzolanic activity of fly ash by strength testing". *Cement and Concrete Research*, Vol. 15, No. 1, 1985. pp. 53-64.
17. Wu, M, Fridh K, Johannesson B & Geiker M: "Impact of sample crushing on porosity characterization of hardened cement pastes by low temperature calorimetry: Comparison of powder and cylinder samples." *Thermochimica Acta,* Vol. 665**,** 2018, pp. 11-19.